RESEARCH ARTICLE

Degree of dopaminergic degeneration measured by ^{99m}Tc-TRODAT-1 SPECT/CT imaging

Ling Lin[1, 2], Jing Ye[2], Han Zhang[2], Zhong-Fu Han[2], Zhi-Hong Zheng[1, 2, *]
1 Fujian Provincial Key Laboratory of Neuroglia and Disease, Fujian Medical University, Fuzhou, Fujian Province, China
2 Department of Biochemistry and Molecular Biology, Fujian Medical University, Fuzhou, Fujian Province, China

Funding: *This study was supported by the National Natural Science Foundation of China, No. 81571250.*

Graphical Abstract

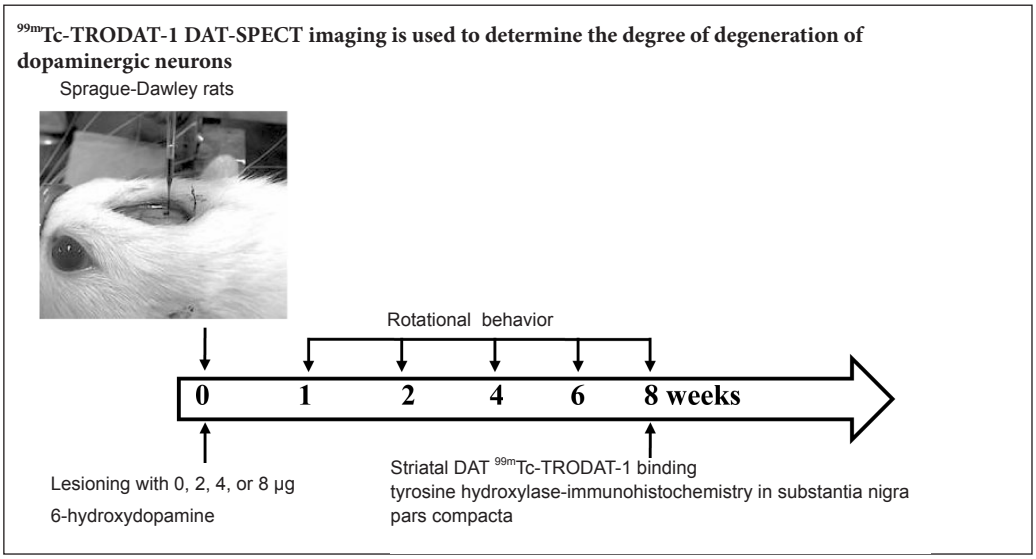

Correspondence to:
Zhi-Hong Zheng, M.D., zhzheng@mail.fjmu.edu.cn.

orcid:
0000-0002-6638-6896 (Zhi-Hong Zheng)

doi: *10.4103/1673-5374.235077*

Accepted: *2018-05-20*

Abstract

To prevent and treat Parkinson's disease in its early stages, it is essential to be able to detect the degree of early dopaminergic neuron degeneration. Dopamine transporters (DAT) in the striatum regulate synaptic dopamine levels, and striatal ^{99m}Tc-TRODAT-1 single-photon emission computed tomography (-SPECT) imaging is a marker for presynaptic neuronal degeneration. However, the association between the degree of dopaminergic degeneration and *in vivo* ^{99m}Tc-TRODAT-1 SPECT imaging is unknown. Therefore, this study investigated the association between the degree of 6-hydroxydopamine (6-OHDA)-induced dopaminergic degeneration and DAT imaging using ^{99m}Tc-TRODAT-1 SPECT in rats. Different degrees of nigrostriatal dopamine depletion were generated by injecting different doses of 6-OHDA (2, 4, and 8 μg) into the right medial forebrain bundle. The degree of nigrostriatal dopaminergic neuron degeneration was assessed by rotational behavior and immunohistochemical staining. The results showed that striatal ^{99m}Tc-TRODAT-1 binding was significantly diminished both in the ipsilateral and the contralateral sides in the 4 and 8 μg 6-OHDA groups, and that DAT ^{99m}Tc-TRODAT-1 binding in the ipsilateral striatum showed a high correlation to apomorphine-induced rotations at 8 weeks post-lesion (r = –0.887, P < 0.01). There were significant correlations between DAT ^{99m}Tc-TRODAT-1 binding in the ipsilateral striatum and the amount of tyrosine hydroxylase immunoreactive neurons in the ipsilateral substantia nigra in the 2, 4, and 8 μg 6-OHDA groups at 8 weeks post-lesion (r = 0.899, P < 0.01). These findings indicate that striatal DAT imaging using ^{99m}Tc-TRODAT-1 is a useful technique for evaluating the severity of dopaminergic degeneration.

Key Words: *nerve regeneration; Parkinson's disease; 6-hydroxydopamine; dopaminergic degeneration; dopamine transporter; ^{99m}Tc-TRODAT-1; tyrosine hydroxylase; substantia nigra; striatum; single-photon emission computed tomography; apomorphine; neurodegeneration; neural regeneration*

Introduction

Parkinson's disease (PD) is a neurodegenerative disorder in which the primary motor symptoms are associated with a progressive loss of dopamine (DA) in the nigrostriatal pathway. Clinically, the typical motor symptoms of PD do not appear until approximately 50–60% of the nigral DA neurons have been destroyed (Liu et al., 2017) and striatal DA has been depleted by 70–80% (Bezard et al., 2001; Stoessl, 2011; Willard et al., 2015; Barber et al., 2017; Segura-Aguilar, 2017). Although several molecular imaging techniques have recently been used to evaluate neuronal loss in clinical PD, including positron emission tomography and single-photon emission computerized tomography (SPECT) (Stoessl, 2011; Bor-Seng-Shu et al., 2014; Joutsa et al., 2015; Niñerola-Baizán et al., 2015; Suwijn et al., 2015), it is difficult to differentiate between tremor-dominant PD and other forms of tremor. Moreover, because there are relatively limited structural changes in the early stages of PD (Stoessl, 2011;

Pagano et al., 2016), the identification of neurodegeneration as early as possible, particularly during the premotor phase, is essential for the prevention and treatment of the disease.

Several researchers have noted that dopamine transporters (DAT) in the striatum regulate synaptic DA levels and affect locomotor activity in PD (Huang et al., 2003; Chotibut et al., 2012; Niñerola-Baizán et al., 2015; Suwijn et al., 2015). In addition, dopaminergic (DAergic) neuron degeneration in the substantia nigra pars compacta (SNc) results in a decrease in the density of DAT in the striatum (Bor-Seng-Shu et al., 2014; Kawaguchi et al., 2016). DAT binding can be used to assess DA function (Stoessl, 2011; Ba and Martin. 2015; Georgiopoulos et al., 2015; Suwijn et al., 2015; Badoud et al., 2016; Caminiti et al., 2017), and SPECT scans using ^{99m}Tc-TRODAT-1 (a ^{99m}Tc-labeled tropane derivative) can be used to image DAT (Wu et al., 2011; Shinto et al., 2014; Huang et al., 2015). Therefore, a measurement of DAT density in the DA nerve terminal can indicate the severity of DA neuronal loss. Although the decrease in striatal DAT density has been described in clinical PD patients (Cummings et al., 2011; Bor-Seng-Shu et al., 2014; Saari et al., 2017) and ^{99m}Tc-TRODAT-1 SPECT imaging has been demonstrated as a useful method for diagnosing PD in its early stages (Wu et al., 2011), few reports have been published regarding the association between the degree of 6-hydroxydopamine (6-OHDA)-induced DAergic degeneration and *in vivo* ^{99m}Tc-TRODAT-1 SPECT/computed tomography (CT) imaging in rats.

In the present study, DAT imaging was used with ^{99m}Tc-TRODAT-1 SPECT/CT to evaluate DAT density in the striatum of unilaterally 6-OHDA-lesioned rats. To mimic the progressive neuronal loss in PD patients, different degrees of nigrostriatal DA depletion were generated by injecting different doses of 6-OHDA. The severity of the lesions was tested by monitoring animal motor behavior and using tyrosine hydroxylase (TH) immunohistochemistry.

Materials and Methods

Animals

A total of 32 male adult Sprague-Dawley rats aged 8–10 weeks and weighing 295–310 g were purchased from Shanghai SLAC Laboratory Animal Co., Ltd. (Shanghai, China; license no. SCXK [Hu] 2012-0001). All rats were housed in a controlled environment at 23 ± 2°C with humidity at 55 ± 5% in a 12-hour light/dark cycle, and were supplied with standard rat chow and drinking water ad libitum. All procedures were approved by the Laboratory Animal Welfare & Ethics of Fujian Medical University of China (approval No. 2015-26).

Of the 32 rats used in this study, 2 died during the experiment. Thirty rats were divided into five groups (n = 6 per group): control, vehicle, and 2, 4, or 8 μg 6-OHDA groups.

Nigrostriatal 6-OHDA lesion

Lesioning with 6-OHDA (6-OHDA hydrochloride, Sigma-Aldrich, St. Louis, MO, USA) was performed as previously described (Meng et al., 2015), with minor modifications. Briefly, rats were anesthetized with 100 mg/kg chloral hydrate through intraperitoneal injection before surgery, and were immobilized in a stereotaxic frame to target the right medial forebrain bundle at the following coordinates relative to the bregma, according to the Paxinos and Watson (2006) rat brain atlas: anterior–posterior: –4.4 mm, medial–lateral: –1.4 mm, and dorsal–ventral: +8.5 mm. To reduce brain damage and allow precise targeting into the medial forebrain bundle, a modified injection procedure was used according to a previous study (Gonzalez-Perez et al., 2010). Briefly, the solution was delivered by a glass capillary needle with a diameter of 100 μm, which was mounted on a microinjection pump connected to a 5 μL Hamilton syringe *via* polyethylene tubing with a diameter of 1 mm. The 2, 4, or 8 μg of 6-OHDA in a total of 2 μL in 0.02% ascorbic acid was infused with a glass capillary needle at a rate of 1 μL/min. The needle was left in place for an additional 10 minutes for maximal diffusion. Lesions were not induced in the control group; however, the vehicle groups were infused with 2 μL of saline containing 0.02% ascorbic acid in an identical manner to the 2, 4, or 8 μg 6-OHDA groups.

Apomorphine-induced rotational behavior

To assess the severity of 6-OHDA-induced DAergic degeneration, apomorphine-induced contralateral rotational behavior was monitored after a single injection of apomorphine (0.5 mg/kg, intraperitoneally; Sigma-Aldrich) at 1, 2, 4, 6, and 8 weeks post-6-OHDA infusion (*i.e.*, behavioral tests were repeated five times). After 5 minutes of apomorphine injection, individual rats were placed in a plastic container that had a circumference and depth of 35 and 15 cm, respectively. The number of rotations was video recorded, and the rotations were counted for 30 minutes.

Preparation of ^{99m}Tc-TRODAT-1 and SPECT/CT imaging

The TRODAT-1 kit was produced by the Institute of Jiangsu Atomic Medicine (Wuxi, China). A dried sample of TRODAT-1 was reconstituted with 2 mL freshly eluted sodium pertechnetate ^{99m}TcO4-, and heated at 100°C for 30 minutes. After cooling to room temperature, the radiochemical quality was tested by thin layer chromatography. Methylbenzene and acetonitrile at a ratio of 80:20 were used as the mobile phase, and the distribution of radioactivity was determined by a thin layer chromatography scanner (Mini-Scan). The radiochemical purity was over 90%.

Eight weeks after 6-OHDA injection, rats under isoflurane (2%) anesthesia were injected with ^{99m}Tc-TRODAT-1 (148–185 MBq/300 μL) *via* the tail vein. The changes in DAT density in the striatum were detected by a nanoScan SPECT/CT preclinical imager (Mediso, Budapest, Hungary). Rats maintained spontaneous breathing during the scan. CT data were acquired using an x-ray voltage biased to 50 kVp with a 670 μA anode current, and the projections were 720°. At 30 minutes post injection, SPECT images were acquired with low-energy, high-resolution collimators. Emission data were acquired in a 256 × 256 matrix size through 360° rotation at 15° intervals for 30 seconds per angle step.

Distribution of ^{99m}Tc-TRODAT-1 in the striatum

SPECT images (Mediso, Budapest, Hungary) were reconstructed with Tera-TomoTM software (Mediso, Budapest, Hungary), and processing and quantification were performed using VivoQuant^{TM} software (Boston, MA, USA). For the analysis of striatal ^{99m}Tc-TRODAT-1 binding, the reconstructed image with the highest signal in the striatum was summed together with its two adjacent slices as a single composite image. Regions of interest were drawn in the striatum in each hemisphere. The DAT radioactivity [^{99m}Tc-TRODAT-1 binding (bq/mm^3)] was counted and corrected for background activity from the cerebellum. All images were examined by two observers who were blinded to the identities of the subject and group.

TH immunohistochemistry

After SPECT imaging, the degree of DAergic neuron loss in the SNc was confirmed by immunohistochemistry. Rats were anesthetized with an overdose of pentobarbital (90 mg/kg, intraperitoneally) and intracardially perfused with 100 mL 0.9% saline solution, followed by 150 mL 4% paraformaldehyde. The entire midbrain was post-fixed for 24 hours in 4% paraformaldehyde in 0.1 M phosphate-buffered saline (PBS) and embedded in paraffin. Coronal sections 5 μm thick were mounted on poly-L-ornithine-coated (Sigma-Aldrich) glass slides. TH immunostaining was used to identify DAergic neurons in the SNc. Briefly, sections were treated with 0.3% hydrogen peroxide for 20 minutes to quench endogenous peroxidase activity, and then blocked with 5% normal goat serum in PBS for 30 minutes. Sections were then incubated with mouse anti-TH monoclonal antibody (1:1000; Millipore, Bedford, MA, USA) overnight at 4°C. After washing with PBS, the sections were incubated with peroxidase-labeled anti-mouse IgG secondary antibody (1:200; Boster, Wuhan, China) at room temperature for 1 hour. After rinsing with PBS, staining was visualized using 3,3-diaminobenzidine (Boster) as the chromogen.

TH-positive neurons were counted under a light microscope (Olympus, Tokyo, Japan) at 20× magnification. For quantification of DA depletion, three adjacent sections were counted per animal, which were selected from the substantia nigra at the level of the optic nerve. Imaging was performed on a Motic microscope system (Motic BA600-4) equipped with a Moticam Pro 285A camera (Olympus), and TH-positive neurons in the SNc of both hemispheres were counted in a blinded fashion.

Statistical analysis

All data are expressed as the mean ± SD. All statistical analyses were performed using SPSS 17.0 software (IBM, Armonk, NY, USA). Data between groups were analyzed using two-way analysis of variance. Significant differences were determined by Tukey's *post hoc* tests. The effects of the 6-OHDA-induced lesion between the ipsilateral and contralateral sides were determined by a paired *t*-test. The correlations between DAT density and TH-positive neurons or apomorphine-induced rotations were analyzed using the Pearson's correlation test. A value of $P < 0.05$ was considered statistically significant.

Results

Apomorphine-induced rotational behavior

Apomorphine-induced contralateral rotation is a reliable indicator of nigrostriatal DA depletion. As shown in **Figure 1**, there were no statistically significant differences among the control, vehicle, and 2 μg 6-OHDA groups. However, the rotational behavior in the 4 μg and 8 μg 6-OHDA groups was significantly higher than in the control group ($P < 0.01$).

DAT binding of ^{99m}Tc-TRODAT-1 in the striatum measured by nanoScan SPECT/CT

As indicated in **Figure 2**, a unilateral injection of 6-OHDA resulted in a significant decrease in striatal ^{99m}Tc-TRODAT-1 binding (bq/mm^3), both in the contralateral (unlesioned, $P < 0.05$) and the ipsilateral (lesioned, $P < 0.01$) sides, in the 4 and 8 μg 6-OHDA groups compared with the corresponding side in the control or vehicle group at 8 weeks post-lesion ($P < 0.05$). When lesions were induced by 2 μg 6-OHDA, the amount of ^{99m}Tc-TRODAT-1 binding on the ipsilateral side was significantly reduced compared with the same side in the control group ($P < 0.01$). There was no significant difference in ^{99m}Tc-TRODAT-1 binding between each side of the striatum in the control or vehicle groups. Representative images are shown in **Figure 3**.

TH-immunoreactive neurons in the SNc

At 8 weeks post-lesion, the remaining numbers of TH-immunoreactive neurons in the ipsilateral SNc were significantly lower than those on the contralateral side($P < 0.01$). Injections of 6-OHDA thus resulted in the loss of TH-immunoreactive neurons in the ipsilateral SNc compared with the contralateral side (**Figure 4A–D**). A significant decrease in the numbers of TH-immunoreactive neurons in both the ipsilateral and contralateral ($P < 0.05$) SNc was found in the 8 μg 6-OHDA group compared with the control group. There was no significant difference in the numbers of TH-immunoreactive neurons between the control and vehicle groups (**Figure 4E**).

Correlation between DAT radioactivity and numbers of TH-immunoreactive neurons

As shown in **Figure 5**, there was a positive correlation between DAT radioactivity in the ipsilateral striatum and the numbers of TH-immunoreactive neurons in the ipsilateral SNc at 8 weeks post-lesion. The Pearson's correlation coefficient was 0.899 at the 0.01 level ($n = 30$).

Correlation between DAT radioactivity and apomorphine-induced rotations

Because there were no significant differences in apomorphine-induced rotations among the control, vehicle, and 2 μg 6-OHDA groups, correlation analysis was only performed between the 4 and 8 μg 6-OHDA groups. As indicated in **Figure 6**, there was a negative correlation between

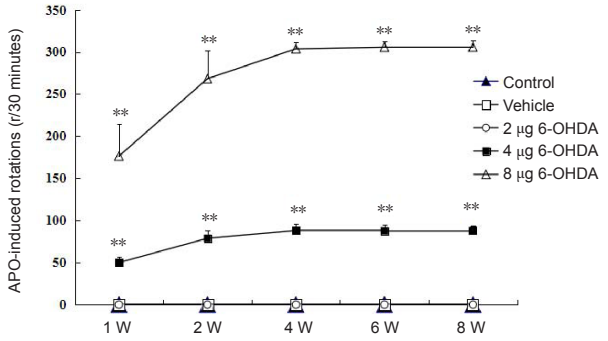

Figure 1 Apomorphine (APO)-induced rotational behavior in rats.
The numbers of rotations towards the contralateral side to the 6-hydroxydopamine (6-OHDA) injection within 30 minutes were recorded at 1, 2, 4, 6, and 8 weeks post-lesion. $^{**}P < 0.01$, *vs.* control group (mean ± SD, $n = 6$; two-way analysis of variance followed by Tukey's *post hoc* test).

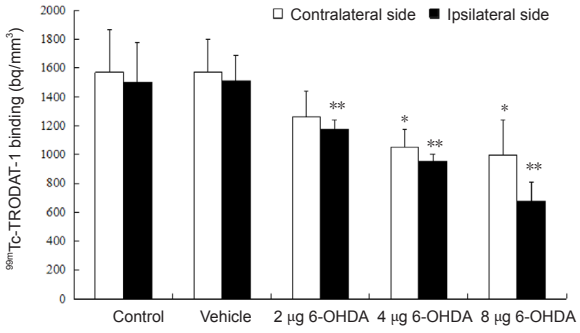

Figure 2 6-Hydroxydopamine (6-OHDA)-induced changes in striatal dopamine transporter (DAT) radioactivity at 8 weeks post-lesion.
DAT radioactivity (^{99m}Tc-TRODAT-1 binding) in the striatum was measured in the 2 μg, 4 μg, and 8 μg 6-OHDA groups and in the control group. $^{*}P < 0.05$, $^{**}P < 0.01$, *vs.* control group (corresponding side) (mean ± SD, $n = 6$; two-way analysis of variance followed by Tukey's *post hoc* test).

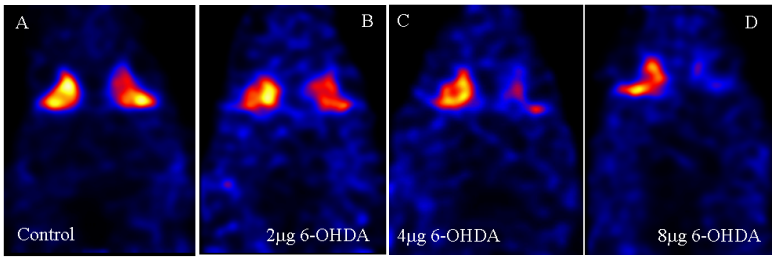

Figure 3 Representative SPECT images of striatal ^{99m}Tc-TRODAT-1 binding at 8 weeks post-lesion.
A relatively symmetrical uptake was observed in the striatum in the control group (A). DAT with ^{99m}Tc-TRODAT-1 binding gradually decreased on the ipsilateral side as the dose of 6-OHDA increased (B–D). Arrows indicate decreased ^{99m}Tc-TRODAT-1 binding. SPECT: Single-photon emission computed tomography; 6-OHDA: 6-hydroxydopamine; DAT: dopamine transporter.

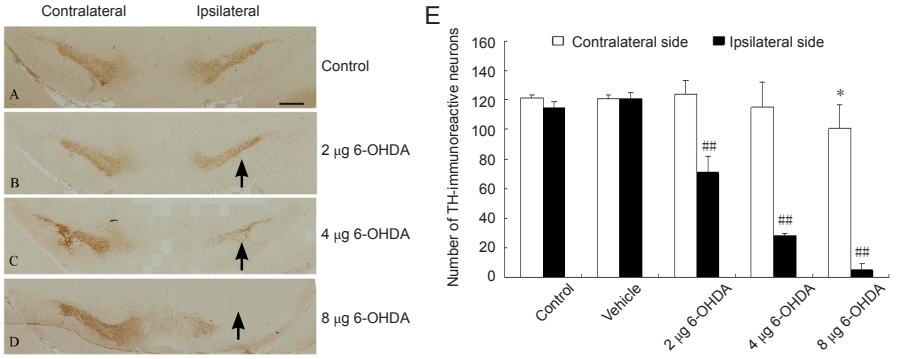

Figure 4 Changes in the numbers of TH-immunoreactive neurons in the substantia nigra pars compacta after 6-OHDA-induced injury.
(A–D) Representative images of tyrosine hydroxylase (TH)-immunoreactive neurons at 8 weeks post-lesion: Rats were injected with saline (A) or different doses of 6-OHDA (B–D). The remaining numbers of TH-immunoreactive neurons were imaged in the substantia nigra pars compacta at 8 weeks post-lesion. Arrows indicate a gradual decrease in TH-immunoreactive neurons. Scale bar: 500 μm. (E) Histogram representing dopaminergic cell loss determined by the quantification of TH-positive neurons in the substantia nigra pars compacta at 8 weeks post-lesion. $^{*}P < 0.05$, *vs.* control group (mean ± SD, $n = 6$; two-way analysis of variance followed by Tukey's *post hoc* test). $^{\#\#}P < 0.01$, *vs.* corresponding side in the same group (mean ± SD, $n = 6$; paired *t*-test). 6-OHDA: 6-Hydroxydopamine; TH: tyrosine hydroxylase.

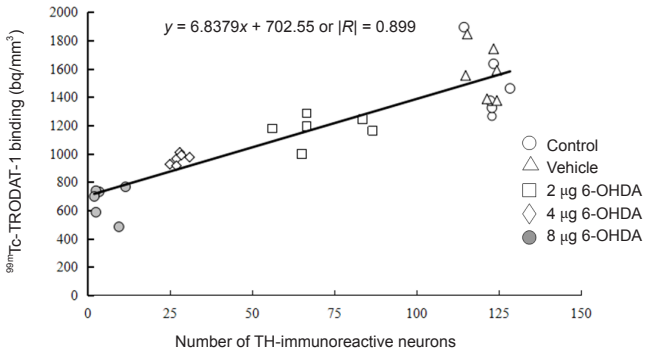

Figure 5 Correlation between DAT ^{99m}Tc-TRODAT-1 binding and TH-immunoreactive neurons.
DAT ^{99m}Tc-TRODAT-1 binding in the ipsilateral striatum was positively correlated to TH-immunoreactive neuron number in the ipsilateral substantia nigra pars compacta at 8 weeks post-lesion. The Pearson's correlation coefficient (R) is shown ($r = 0.899$, $P < 0.01$, $n = 30$). DAT: Dopamine transporter; TH: tyrosine hydroxylase.

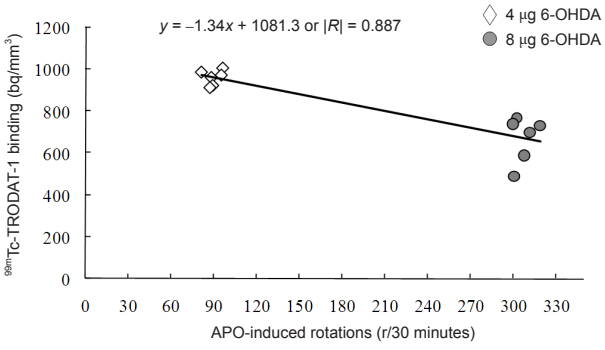

Figure 6 Correlation between DAT ^{99m}Tc-TRODAT-1 binding and APO-induced rotations.
DAT ^{99m}Tc-TRODAT-1 binding in the ipsilateral striatum showed a high correlation with APO-induced rotations at 8 weeks post-lesion (4 and 8 μg 6-OHDA groups). The Pearson's correlation coefficient (R) is shown ($r = 0.887$, $P < 0.01$, $n = 12$). DAT: Dopamine transporter; 6-OHDA: 6-hydroxydopamine; APO: apomorphine.

DAT radioactivity in the ipsilateral striatum and apomorphine-induced rotations at 8 weeks post-lesion. The Pearson's correlation coefficient was −0.887 at the 0.01 level (n = 12).

Discussion

The present study investigated the relationship between 6-OHDA-induced DAergic degeneration and DAT imaging using ^{99m}Tc-TRODAT-1 SPECT/CT.

6-OHDA is widely used to induce degeneration of midbrain DA neurons to create animal models of PD (Duty and Jenner, 2011; Blesa et al., 2012; Bäck et al., 2013; Le et al., 2014). Our behavioral studies showed that although both the 4 and 8 μg 6-OHDA groups responded to apomorphine with significantly increased numbers of rotations, the number of rotations in the 4 μg 6-OHDA group was < 86 turns/30 minutes at 1–8 weeks post-lesion. However, the rotational response in the 8 μg 6-OHDA group was > 264 turns/30 minutes at 2 weeks post-lesion, and the rotational frequency increased a further 15% during 4–8 weeks post-lesion. These findings are similar to those from previous research, which showed that injecting increasing concentrations of 6-OHDA into the medial forebrain bundle can produce behavioral changes in a dose-dependent manner (Truong et al., 2006). This result also supports the idea that apomorphine-induced rotational behavior is not sensitive enough to detect partial lesions (Boix et al., 2015).

Pathologically, PD is characterized by the loss of DAergic neurons in the SNc that primarily project to the striatum (Shi and Chen, 2017). Our data indicate significant changes in rotational asymmetry following administration of apomorphine (with DAergic neuron loss approximately 70% in the SNc), which is in agreement with the findings of prior studies in rats with DAergic neuron loss of > 50% (Hefti et al., 1980; Hudson et al., 1993). However, our results differ from findings by other researchers showing that apomorphine-induced rotations resulted from DAergic neuron losses as low as 40% (Przedborski et al., 1995; Truong et al., 2006). This inconsistency could result from variations in experimental design, such as the duration of behavioral tests (Gui et al., 2011) and the concentration of apomorphine used.

Some studies have suggested that, in rat PD models, chronic injections of the DA receptor agonist R-apomorphine provide neuroprotective effects (Yuan et al., 2004; Gui et al., 2011). In the current study, apomorphine-induced behavioral tests were repeated five times (at 1, 2, 4, 6, and 8 weeks after 6-OHDA injection). There were no obvious protective effects under our experimental conditions. A possible explanation is that the anti-parkinsonian effects of apomorphine are largely dependent on experimental procedures. Although rats received apomorphine five times in this study, each time only 0.5 mg/kg was injected intraperitoneally. In contrast, Yuan et al. (2004) and Gui et al. (2011) used R-apomorphine (10 mg/kg per day subcutaneously) for 11 consecutive days.

DAT is located in presynaptic DAergic nerve terminals, and plays a critical role in removing DA from the synaptic cleft and in regulating extracellular DA concentrations (Shen et al., 2012; Tian et al., 2012). Therefore, the density of DAT in the striatum may represent a presynaptic DAergic function. Because DAT is selectively expressed by DA neurons, specific SPECT ligands for DAT imaging (FP-CIT, beta-CIT, IPT, TRODAT-1) provide a marker for presynaptic neuronal degeneration (Goebel et al., 2011; Bor-Seng-Shu et al., 2014; Hsiao et al., 2014). ^{99m}Tc-TRODAT-1 is a recently developed radiotracer that selectively binds to DAT (Wang et al., 2012). There was only a marked reduction in the ipsilateral striatal DAT uptake with 2 μg 6-OHDA in the present study. It could be that injection with 4 and 8 μg of 6-OHDA reduces DAT uptake progressively in both the contralateral and ipsilateral striatum. However, the increase over time in apomorphine-induced rotations indicates that damage to DAergic neurons is largely unilateral. The reasons for this inconsistency between apomorphine-induced behavior and DAT uptake need to be studied further.

Our results showed agreement between the distribution of ^{99m}Tc-TRODAT-1 in the ipsilateral striatum and the remaining TH-positive neurons in the SNc, indicating that reduced DAT binding corresponds with a loss of DAergic neurons. This result is in line with previous studies from animal and clinical studies, showing that a decrease of DAergic neurons in the SNc may lead to a reduction of DAT uptake in the striatum (Bäck et al., 2013; Bor-Seng-Shu et al., 2014; Kraemmer et al., 2014). However, the opposite result has been reported recently by others, who found that postmortem SNc neuron numbers had no relationship with striatal DAT binding in PD patients (Saari et al., 2017). This inconsistency may partly be explained by the loss of DAergic neurons in the SNc in late-stage PD, which is associated with other factors such as a loss of co-transmitter release from DA neurons, inflammatory responses, and gliosis (Seutin, 2005; Nagatsu and Sawada, 2006; Whitton, 2007). Moreover, it is difficult to show a close relationship between biomarker changes over time and changes in severity in clinical PD (Stoessl et al., 2014), especially when the degeneration of SNc neurons and striatal DA is greater than 50% (Saari et al., 2017). Although DAT density, visualized using ^{99m}Tc-TRODAT-1 binding, was remarkably decreased in the bilateral striatum in both the 4 and 8 μg 6-OHDA groups after 8 weeks, increasing concentrations of 6-OHDA tended to decrease DAT uptake from the 2 μg 6-OHDA group, in which the mean DA neuron loss was approximately 40%. This supports the idea that ^{99m}Tc-TRODAT-1/SPECT imaging may detect nigrostriatal DA neuronal degeneration in the early stages of PD, and that this imaging technique may be of use to assess the severity of nigrostriatal DA neuronal degeneration.

It is also important to note that the correlation between the number of DAergic neurons and SPECT results was strong, because there were large differences between groups (control, low, and high dose of 6-OHDA). This is similar to in the clinical situation, where the DaT-SCAN works well to differentiate PD patients from controls (Stoessl, 2011; Suwijn et al., 2015). In contrast, the correlation within groups (*e.g.*, the 4 μg or 8 μg group) between the number of TH-positive

neurons and SPECT results was poor. This is consistent with clinical data that suggests that the DaT-SCAN is not suitable for monitoring disease progression (Saari et al., 2017).

Some clinical studies have suggested that there is a more marked reduction of striatal DAT binding on the contralateral side to the more affected limbs than on the ipsilateral side (Huang et al., 2001; Booth et al., 2015); however, there was no significant difference in ^{99m}Tc-TRODAT-1 binding between the contralateral and ipsilateral sides in this study. In the present study, both DAT binding in the striatum and TH-immunoreactivity in the SNc were bilaterally impaired after a unilateral injection of 8 μg 6-OHDA to the medial forebrain bundle (there was a loss of approximately 95% of DAergic neurons, similar to what is observed in advanced PD). This finding indicates that severe unilateral ablation of DA neurons might impair the bilateral nigrastriatal pathway. This phenomenon may reflect the dysfunction in striatal DA homeostasis in the later stages of PD. It is worth noting that the approximately 75% decrease in TH-immunoreactivity in the 4 μg 6-OHDA group reported in the present study is higher than that of a previous study (Truong et al., 2006). This discrepancy may be associated with our modified injection procedure, which significantly improves accuracy.

The correlations between DAT radioactivity and apomorphine-induced rotations or TH-immunoreactive neuron numbers further supports the idea that PD symptoms are associated with both a loss of DA neurons in the SNc and a reduction of DAT uptake in the striatum.

The limitations of the present study are: (1) We did not differentiate ^{99m}Tc-TRODAT-1 binding in the subregions of the striatum (such as the caudate or putamen), and (2) the small size of the animals for ^{99m}Tc-TRODAT-1 binding. It would be helpful for future studies to increase the sample size, and to observe ^{99m}Tc-TRODAT-1 binding in different subregions of the striatum in detail.

In conclusion, our data support the use of DAT imaging with ^{99m}Tc-TRODAT-1 SPECT for the diagnosis of early PD In the future, earlier diagnosis of PD using this technique may allow for presymptomatic intervention.

Acknowledgments: *We thank Dr. Wen-Xin Chen from Fujian Provincial Hospital of China for providing TRODAT-1 reagent, and staff from the Center for Molecular Imaging in Xiamen University of China for their professional technical assistance.*
Author contributions: *LL, JY and ZHZ conceived and designed the experiments, analyzed the data, and wrote the paper. JY, HZ and ZFH performed the experiments. ZHZ and LL contributed reagents/materials/analysis tools. All authors approved the final version of the paper.*
Conflicts of interest: *The authors declare no competing financial interests.*
Financial support: *This study was supported by the National Natural Science Foundation of China, No. 81571250. The funder did not participant in the study design, in the collection, analysis and interpretation of data, in the writing of the paper, and in the decision to submit the paper for publication.*
Institutional review board statement: *This study was approved by the Laboratory Animal Welfare & Ethics in Fujian Medical University (2015-26). The experimental procedure followed the United States National Institutes of Health Guide for the Care and Use of Laboratory Animals (NIH Publication No. 85-23, revised 1985).*
Copyright license agreement: *The Copyright License Agreement has been signed by all authors before publication.*
Data sharing statement: *Datasets analyzed during the current study are available from the corresponding author on reasonable request.*
Plagiarism check: *Checked twice by iThenticate.*
Peer review: *Externally peer reviewed.*

Open peer reviewer: *Peng Luo, Fourth Military Medical University, China.*
Additional file: *Open peer review report 1.*

References

Ba F, Martin WR (2015) Dopamine transporter imaging as a diagnostic tool for parkinsonism and related disorders in clinical practice. Parkinsonism Relat Disord 21:87-94.

Badoud S, Van De Ville D, Nicastro N, Garibotto V, Burkhard PR, Haller S (2016) Discriminating among degenerative parkinsonisms using advanced (123)I-ioflupane SPECT analyses. Neuroimage Clin 12:234-240.

Bäck S, Raki M, Tuominen RK, Raasmaja A, Bergström K, Männistö PT (2013) High correlation between in vivo [123I]β-CIT SPECT/CT imaging and post-mortem immunohistochemical findings in the evaluation of lesions induced by 6-OHDA in rats. EJNMMI Res 3:46.

Barber TR, Klein JC, Mackay CE, Hu MTM (2017) Neuroimaging in pre-motor Parkinson's disease. Neuroimage Clin 15:215-227.

Bellucci A, Mercuri NB, Venneri A, Faustini G, Longhena F, Pizzi M, Missale C, Spano P (2016) Review: Parkinson's disease: from synaptic loss to connectome dysfunction. Neuropathol Appl Neurobiol 42:77-94.

Bezard E, Dovero S, Prunier C, Ravenscroft P, Chalon S, Guilloteau D, Crossman AR, Bioulac B, Brotchie JM, Gross CE (2001) Relationship between the appearance of symptoms and the level of nigrostriatal degeneration in a progressive 1-methyl-4-phenyl-1,2,3,6-tetrahydropyridine-lesioned macaque model of Parkinson's disease. J Neurosci 21:6853-6861.

Blesa J, Phani S, Jackson-Lewis V, Przedborski S (2012) Classic and new animal models of Parkinson's disease. J Biomed Biotechnol 2012:845618.

Boix J, Padel T, Paul G (2015) A partial lesion model of Parkinson's disease in mice-characterization of a 6-OHDA-induced medial forebrain bundle lesion. Behav Brain Res 284:196-206.

Booth TC, Nathan M, Waldman AD, Quigley AM, Schapira AH, Buscombe J (2015) The role of functional dopamine-transporter SPECT imaging in parkinsonian syndromes, part 1. AJNR Am J Neuroradiol 36: 229-235.

Bor-Seng-Shu E, Felicio AC, Braga-Neto P, Batista IR, Paiva WS, de Andrade DC, Teixeira MJ, de Andrade LA, Barsottini OG, Shih MC, Bressan RA, Ferraz HB (2014) Dopamine transporter imaging using ^{99m}Tc-TRODAT-1 SPECT in Parkinson's disease. Med Sci Monit 20:1413-1418.

Caminiti SP, Presotto L, Baroncini D, Garibotto V, Moresco RM, Gianolli L, Volonté MA, Antonini A, Perani D (2017) Axonal damage and loss of connectivity in nigrostriatal and mesolimbic dopamine pathways in early Parkinson's disease. Neuroimage Clin 14:734-740.

Chotibut T, Apple DM, Jefferis R, Salvatore MF (2012) Dopamine transporter loss in 6-OHDA Parkinson's model is Unmet by parallel reduction in dopamine uptake. PLoS One 7:e52322.

Cummings JL, Henchcliffe C, Schaier S, Simuni T, Waxman A, Kemp P (2011) The role of dopaminergic imaging in patients with symptoms of dopaminergic system neurodegeneration. Brain 134:3146-3166.

Duty S, Jenner P (2011) Animal models of Parkinson's disease: a source of novel treatments and clues to the cause of the disease. Br J Pharmacol 164:1357-1391.

Georgiopoulos C, Davidsson A, Engström M, Larsson EM, Zachrisson H, Dizdar N (2015) The diagnostic value of dopamine transporter imaging and olfactory testing in patients with parkinsonian syndromes. J Neurol 262:2154-2163.

Goebel G, Seppi K, Donnemiller E, Warwitz B, Wenning GK, Virgolini I, Poewe W, Scherfler C (2011) A novel computer-assisted image analysis of [123I]β-CIT SPECT images improves the diagnostic accuracy of parkinsonian disorders. Eur J Nucl Med Mol Imaging 38:702-710.

Gonzalez-Perez O, Guerrero-Cazares H, Quiñones-Hinojosa A (2010) Targeting of deep brain structures with microinjections for delivery of drugs, viral vectors, or cell transplants. J Vis Exp doi: 10.3791/2082.

Gui ZH, Liu J, Wang Y, Ali U, Wang T, Chen L (2011) Effects of chronic, systemic treatment with the dopamine receptor agonist R-apomorphine in partially lesioned rat model of Parkinson's disease: an electrophysiological study of substantia nigra dopamine neurons. Chin J Physiol 54:96-104.

Hefti F, Melamed E, Sahakian BJ, Wurtman RJ (1980) Circling behavior in rats with partial, unilateral nigro-striatal lesions: effect of amphetamine, apomorphine, and DOPA. Pharmacol Biochem Behav 12:185-188.

Hsiao IT, Weng YH, Hsieh CJ, Lin WY, Wey SP, Kung MP, Yen TC, Lu CS, Lin KJ (2014) Correlation of Parkinson disease severity and 18F-DTBZ positron emission tomography. JAMA Neurol 71:758-766.

Huang CK, Wu J, Cheng KY, Pan LK (2015) Optimization of imaging parameters for SPECT scans of [99mTc]TRODAT-1 using Taguchi analysis. PLoS One 10:e0113817.

Huang WS, Chiang YH, Lin JC, Chou YH, Cheng CY, Liu RS (2003) Crossover study of (99m)Tc-TRODAT-1 SPECT and (18)F-FDOPA PET in Parkinson's disease patients. J Nucl Med 44:999-1005.

Huang WS, Lin SZ, Lin JC, Wey SP, Ting G, Liu RS (2001) Evaluation of early-stage Parkinson's disease with 99mTc-TRODAT-1 imaging. J Nucl Med 42:1303-1308.

Hudson JL, van Horne CG, Strömberg I, Brock S, Clayton J, Masserano J, Hoffer BJ, Gerhardt GA (1993) Correlation of apomorphine- and amphetamine-induced turning with nigrostriatal dopamine content in unilateral 6-hydroxydopamine lesioned rats. Brain Res 626:167-174.

Joutsa J, Johansson J, Seppänen M, Noponen T, Kaasinen V (2015) Dorsal-to-ventral shift in midbrain dopaminergic projections and increased thalamic/raphe serotonergic function in early Parkinson disease. J Nucl Med 56:1036-1041.

Kawaguchi H, Shimada H, Kodaka F, Suzuki M, Shinotoh H, Hirano S, Kershaw J, Inoue Y, Nakamura M, Sasai T, Kobayashi M, Suhara T, Ito H (2016) Principal component analysis of multimodal neuromelanin MRI and dopamine transporter PET data provides a specific metric for the nigral dopaminergic neuronal density. PLoS One 11:e0151191.

Kraemmer J, Kovacs GG, Perju-Dumbrava L, Pirker S, Traub-Weidinger T, Pirker W (2014) Correlation of striatal dopamine transporter imaging with post mortem substantia nigra cell counts. Mov Disord 29:1767-1773.

Le W, Sayana P, Jankovic J (2014) Animal models of Parkinson's disease: a gateway to therapeutics? Neurotherapeutics 11:92-110.

Liu LX, Du D, Zheng T, Fang Y, Chen YS, Yi HL, He QY, Gao DW, Shi QL (2017) Detecting dopaminergic neuronal degeneration using diffusion tensor imaging in a rotenone-induced rat model of Parkinson's disease: fractional anisotropy and mean diffusivity values. Neural Regen Res 12:1485-1491.

Meng T, Yuan S, Zheng Z, Liu T, Lin L (2015) Effects of endogenous melatonin on glutamate and GABA rhythms in the striatum of unilateral 6-hydroxydopamine-lesioned rats. Neuroscience 286:308-315.

Nagatsu T, Sawada M (2006) Cellular and molecular mechanisms of Parkinson's disease: neurotoxins, causative genes, and inflammatory cytokines. Cell Mol Neurobiol 26:781-802.

Niñerola-Baizán A, Rojas S, Bonastre M, Tudela R, Lomeña F, Pavía J, Marin C, Ros D (2015) In vivo evaluation of the dopaminergic neurotransmission system using [123I]FP-CIT SPECT in 6-OHDA lesioned rats. Contrast Media Mol Imaging 10:67-73.

Niñerola-Baizán A, Rojas S, Roé-Vellvé N, Lomeña F, Ros D, Pavía J (2015) Dopamine transporter imaging in the aged rat: a [^{123}I]FP-CIT SPECT study. Nucl Med Biol 42:395-398.

Pagano G, Niccolini F, Politis M (2016) Imaging in Parkinson's disease. Clin Med (Lond) 16:371-375.

Paxinos G, Watson C (2006) The rat brain in stereotaxic coordinates. San Diego: Academic Press, USA.

Przedborski S, Levivier M, Jiang H, Ferreira M, Jackson-Lewis V, Donaldson D, Togasaki DM (1995) Dose-dependent lesions of the dopaminergic nigrostriatal pathway induced by intrastriatal injection of 6-hydroxydopamine. Neuroscience 67:631-647.

Saari L, Kivinen K, Gardberg M, Joutsa J, Noponen T, Kaasinen V (2017) Dopamine transporter imaging does not predict the number of nigral neurons in Parkinson disease. Neurology 88:1461-1467.

Schulz-Schaeffer WJ (2015) Is cell death primary or secondary in the pathophysiology of idiopathic Parkinson's disease? Biomolecules 5:1467-1479.

Segura-Aguilar J (2017) On the role of endogenous neurotoxins and neuroprotection in Parkinson's disease. Neural Regen Res 12:897-901.

Seutin V (2005) Dopaminergic neurones: much more than dopamine? Br J Pharmacol 146:167-169.

Shen LH, Liao MH, Tseng YC (2012) Recent advances in imaging of dopaminergic neurons for evaluation of neuropsychiatric disorders. J Biomed Biotechnol 2012:259349.

Shi CK, Chen ZQ (2017) Effect of microglia on iron metabolismin midbrain dopaminergic neurons and the underlying mechanism: study protocol for an in vitro cellular experiment. Zhongguo Zuzhi Gongcheng Yanjiu 21:1262-1267.

Shinto AS, Antony J, Kamaleshwaran K, Vijayan K, Selvan A, Korde A, Kameshwaran M, Samuel G (2014) Correlative (99m)tc-labeled tropane derivative single photon emission computer tomography and clinical assessment in the staging of Parkinson disease. World J Nucl Med 13:178-183.

Stoessl AJ (2011) Neuroimaging in Parkinson's disease. Neurotherapeutics 8:72-81.

Stoessl AJ, Lehericy S, Strafella AP (2014) Imaging insights into basal ganglia function, Parkinson's disease, and dystonia. Lancet 384:532-544.

Suwijn SR, van Boheemen CJ, de Haan RJ, Tissingh G, Booij J, de Bie RM (2015) The diagnostic accuracy of dopamine transporter SPECT imaging to detect nigrostriatal cell loss in patients with Parkinson's disease or clinically uncertain parkinsonism: a systematic review. EJNMMI Res 5:12.

Tian L, Karimi M, Loftin SK, Brown CA, Xia H, Xu J, Mach RH, Perlmutter JS (2012) No differential regulation of dopamine transporter (DAT) and vesicular monoamine transporter 2 (VMAT2) binding in a primate model of Parkinson disease. PLoS One 7:e31439.

Truong L, Allbutt H, Kassiou M, Henderson JM (2006) Developing a preclinical model of Parkinson's disease: a study of behaviour in rats with graded 6-OHDA lesions. Behav Brain Res 169:1-9.

Wang L, Zhang Q, Li H, Zhang H (2012) SPECT molecular imaging in PD. J Biomed Biotechnol 2012:412486.

Whitton PS (2007) Inflammation as a causative factor in the aetiology of Parkinson's disease. Br J Pharmacol 150:963-976.

Willard AM, Bouchard RS, Gittis AH (2015) Differential degradation of motor deficits during gradual dopamine depletion with 6-hydroxydopamine in mice. Neuroscience 301:254-267.

Wu H, Lou C, Huang Z, Shi G (2011) SPECT imaging of dopamine transporters with (99m)Tc-TRODAT-1 in major depression and Parkinson's disease. J Neuropsychiatry Clin Neurosci 23:63-67.

Yuan H, Sarre S, Ebinger G, Michotte Y (2004) Neuroprotective and neurotrophic effect of apomorphine in the striatal 6-OHDA-lesion rat model of Parkinson's disease. Brain Res 1026:95-107.

(*Copyedited by Gardner B, Haase R, Wang J, Li CH, Qiu Y, Song LP, Zhao M*)